ELSEVIER

Contents lists available at ScienceDirect

Science Bulletin

journal homepage: www.elsevier.com/locate/scib



Article

Carbonaceous aerogel and CoNiAl-LDH@CA nanocomposites derived from biomass for high performance pseudo-supercapacitor

Sidi Zhang a,b, Jian Liu a,b, Peipei Huang a,b, Hao Wang c, Changyan Cao a,b,*, Weiguo Song a,b,*

- ^a Beijing National Laboratory for Molecular Sciences, Key Laboratory of Molecular Nanostructure and Nanotechnology, CAS Research/Education Center for Excellence in Molecular Sciences, Institute of Chemistry, Chinese Academy of Sciences, Beijing 100190, China
- ^b University of Chinese Academy of Sciences, Beijing 100049, China
- ^c The Academy of Military Economics Student Brigade, Wuhan 430035, China

ARTICLE INFO

Article history: Received 24 February 2017 Received in revised form 18 March 2017 Accepted 26 April 2017 Available online 18 May 2017

Keywords: Biomass Carbonaceous aerogel Layered double hydroxide Supercapacitor

ABSTRACT

Conversion of waste biomass to valuable carbonaceous material is a sustainable and environmental benign method for energy and reduction of greenhouse gas emission. Herein, a two-step hydrothermal method was developed to fabricate high performance electrode material from pomelo peels. In the first step, the pomelo peels were transformed to carbonaceous aerogel (CA), which constructed of three-dimensional, sponge-like brown monolith with hierarchical pores, low-density (0.032 g/cm³) and excellent mechanical flexibility. Then, the cobalt nickel aluminum layered double hydroxide (CoNiAl-LDH) was in situ loaded on the surface of CA to form exquisite core-shell structure (CoNiAl-LDH@CA) through the second hydrothermal step. When used as an electrode material for supercapacitor, CoNiAl-LDH@CA exhibited high specific capacitances of 1,134 F/g at 1 A/g and 902 F/g at 10 A/g, respectively. Furthermore, they displayed an excellent cycling stability without an obvious capacitance decrease after 4,000 cycles.

© 2017 Science China Press. Published by Elsevier B.V. and Science China Press. All rights reserved.

1. Introduction

In order to meet the increasing energy demand and decreasing fossil consumption and environmental pollution requirements, many efforts have been made in order to find high-performance, low-cost and environmentally-friendly energy storage devices [1,2]. Recently, supercapacitor as an electrochemical capacitor has received wide attention, and it has significant advantages of high power density and long cycling life [3]. Based on the charge storage mechanism, supercapacitor can be classified into electrical double-layer capacitor (EDLC) and redox capacitor (pseudo capacitor) [4].

In most cases, porous carbon materials such as activated carbons, carbon nanotubes (CNTs), graphene, carbon fibers, carbon spheres and carbon aerogel have been studied to act as electrode material for EDLC capacitor [5–13]. Although they have high power density and long life span, the relatively low capacitance has limited the commercial application of EDLC capacitor. In spite of the conventional carbon materials, transition metal oxides, hydroxides and conducting redox polymers have also been explored as the

active electrode material [14–21]. Of these electrode materials, layered double hydroxide (LDH) containing transition metal elements (Co²⁺, Ni²⁺) has been considered as one of the most promising alternative electrode material due to its high energy density, low-cost, high stability and versatility in composition and morphology, and highly dispersion degree of active sites [22–24]. However, the poor electrical conductivity and the weakly mechanism stability impeded its application. Therefore, combing LDH and carbonaceous material may be one promising way to improve the specific capacitance of supercapacitor.

Biomass, including glucose, cellulose, lignin biopolymers has been employed as sustainable and renewable material for the synthesis of functional material [7,16,25–27]. Various methods have been established to obtain the carbonaceous materials, such as freezing-thawing, hydrothermal carbonization, high-temperature calcinations [8,15,18,28,29]. As many literatures reported, hydrothermal route is the widely used. In addition, the biomass can be fabricated to be carbonaceous aerogel (CA) directly through one-pot hydrothermal carbonization (HTC) process [30,31]. Herein, we used the HTC approach to synthesize sponge-like carbonaceous aerogel with pomelo peels as the carbon source. The synthesized brown monolith maintains three-dimensional structure in macro scale and forms hierarchical porous nano architecture. Furthermore, we decorated cobalt nickel aluminum layered double

^{*} Corresponding authors.

E-mail addresses: cycao@iccas.ac.cn (C. Cao), wsong@iccas.ac.cn (W. Song).

hydroxides (CoNiAl-LDH) on the surface of CA. The obtained CoNiAl-LDH@CA exhibited excellent electrochemical properties in pseudo capacitor. The specific capacitances reached as high as 1,134 F/g at 1 A/g and 902 F/g at 10 A/g, respectively.

2. Materials and methods

2.1. Synthesis of carbon aerogel

To synthesize the CA, carbonaceous gel (CG) was firstly prepared via a one-pot hydrothermal process directly from pomelo peels. Pomelo peels was cut into different sizes and the yellow peel skin was removed. After keeping in the Teflon-lined stainless steel autoclave for 6.5 h at 180 °C, the wetting gel was obtained and then soaked by deionized water and ethanol for several days to remove soluble impurities. At last, the CA would be obtained after freeze-drying for 2 d at -42 °C.

2.2. Synthesis of CoNiAl-LDH@CA

In a typical synthesis, 6 mmol $Co(NO_3)\cdot 6H_2O$, 4.5 mmol Ni $(NO_3)\cdot 6H_2O$, 3 mmol $Al(NO_3)\cdot 9H_2O$ and 31.5 mmol urea was dissolved in 25 mL anhydrous methanol at room temperature. Then the homogeneous mixed solution was added drop wise onto the as-prepared carbonaceous aerogel with the sizes of 2 cm \times 3 cm \times 3 cm via the plastic dropper. After being saturated with the mixed solution the wet carbonaceous gel was transferred into a 50 mL autoclave and kept at 150 °C for 12 h. Subsequently, the obtained black monolith was immersed into deionized water for 2 d to remove the residual ions absorbed on the surface. Finally, the CoNiAl-LDH@CA was obtained after freeze-drying for 2 d.

2.3. Characterizations

The microscopic features of the samples were characterized by scanning electron microscopy (SEM, JEOL-6701F) and transmission electron microscopy (TEM, JEOL JEM-2100F, 100 kV). X-ray powder diffraction (XRD) patterns were collected on an X-ray diffractometer (Rigaku D/max-2500 diffractometer with Cu K α radiation, λ = 0.154056 nm) at 40 kV and 200 mA. The surface area of the products was measured by the Brunauer-Emmett-Teller (BET) method using N_2 adsorption and desorption isotherms on an Autosorb-1 analyzer at 78.3 K. Fourier transformed infrared (FT-IR) spectra were record on a Nicolet Magana-IR 750 spectrometer over a range from 400 to 4,000 cm $^{-1}$. Raman spectra were obtain using a Thermo Scientic DXR Raman Microscope with 532 nm laser as an excitation source. X-ray photoelectron spectroscopy (XPS) was performed on the VG Scientific ESCALab220i-XL spectrometer using Al K α radiation.

2.4. Electrochemical measurement

All the electrochemical measurements were carried out in the CHI660D electrochemical working station at room temperature and a platinum foil and a saturated calomel electrode (SCE) were used as counter and reference electrodes, respectively. The working electrodes were prepared by dissolve electro active material (the as-prepared samples) 80%, super-p 10% and teflonized acetylene black (TAB) 10% in ethanol, stirred 12 h to form a slurry. After coating the above slurries on foamed Ni grids, the electrodes were dried at 60 °C for several hours before pressing under a pressure of 6 MPa. Each electrode contained about 2 mg of electro active material. Cyclic voltammetry (CV) curve were performed between 0.15 and 0.55 V (vs. SCE) by various-scanning rates at 5–100 mV. Galvanostatic charge/discharge curves were measured in the

potential range of 0.15 to 0.55 V (vs. SCE) at different current density of 1-10~A/g.

3. Results and discussion

CA was first obtained under hydrothermal of pomelo peels directly. During this HTC process, a series of polymerization-poly condensation reactions occurred and formed a black cross-linked structure carbonaceous gel with rough surface [31]. After washed with ethanol and deionized water and the freeze-drying process, the black wet hydrogel turned to brown dry aerogel with porous structure. The obtained carbonaceous aerogel looked like a light sponge-like monolith, which could be compressed and recovered to its initial stage. The density of CA was measured to be 0.032 g/cm³ (Fig. 1a). In addition, it owned good hydrophilicity and a robust structure (Fig. 1b-d), which will facilitate the following load of LDHs.

In the second step, the mixed metal ions solution was added drop by drop to the CA surface until saturated. Then, the wet hydrogel with metal ion was heated to 150 °C and kept for 12 h. During this process, urea was decomposed slowly to provide OHgradually, enabling the metal ion to form CoNiAl-LDH [22]. Eventually, the nano sheet like CoNiAl-LDH was grown on the surface of CA [32]. After freeze-drying, the light monolithic with promising electrochemical properties was obtained. As shown in Fig. 2, the as-prepared CoNiAl-LDH@CA preserved the three-dimensional porous structure with nano scale LDH nanosheets perpendicularly grown on the surface of CA, leading to a lumpy appearance. For comparison, only flower-like CoNiAl-LDH spheres were obtained without CA (Fig. S1 online), indicating that CA played an important role during this synthesis process. The EDS mapping was used to detect the elemental distribution of CoNiAl-LDH@CA (Fig. 2c). The images demonstrated that Co, Ni and Al had a uniform and continuous dispersion throughout CA, indicating that the LDH sheets were on the surface of CA. The XRD patterns of CoNiAl-LDH@CA are presented in Fig. 3. The diffraction peaks exhibited characteristic reflections of (003), (006), (012), (015) and (110), which can be assigned to the layer structure of LDH. No other crystalline phase can be observed.

It can be concluded that CA not only provided anchors for transition metal ions to forming LDH nanosheets, but also effectively

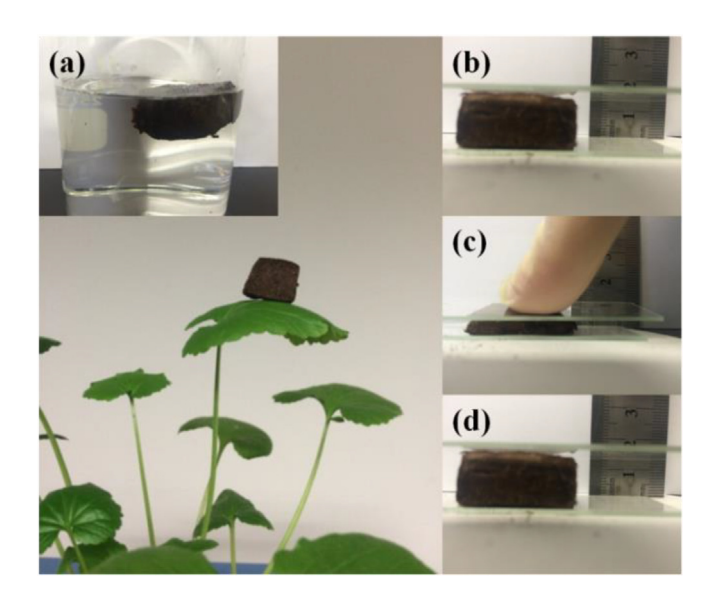


Fig. 1. (Color online) (a) The low-density of CA, (b-d) the compression and recovery of CA.

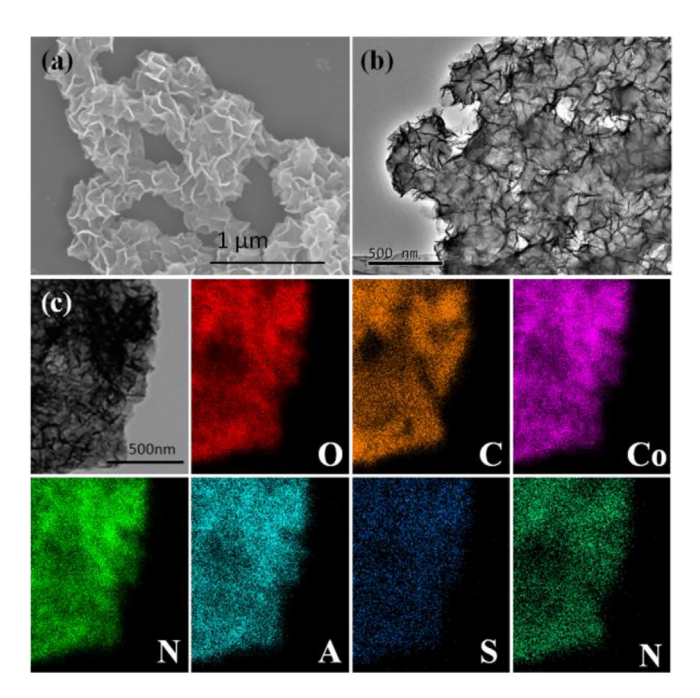


Fig. 2. (Color online) (a) SEM image, (b) TEM image, (c) EDS elemental mapping image of CoNiAl-LDH@CA.

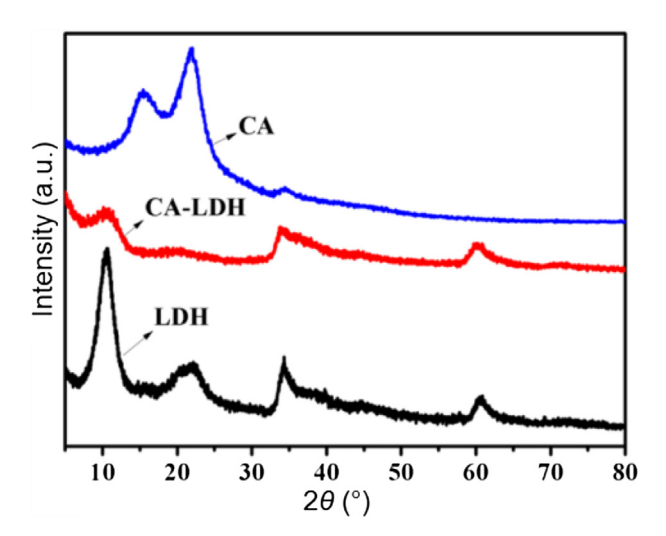


Fig. 3. (Color online) XRD patterns of CA, CoNiAl-LDH@CA and CoNiAl-LDH.

dispersed LDH nanosheets to expose more electroactive sites and increasing the surface area of the composite. In order to investigate how this CoNiAl-LDH shell can grow in the surface of CA, Fourier transform infrared (FT-IR) spectroscopy and X-ray photoelectron spectroscopy (XPS) were used to identify the surface group of CA (Fig. S2 online). From the FT-TR spectrum, the band at 3,422 cm⁻¹ was attributed to O—H stretching vibration and the band at 2,925 cm⁻¹ was C—H symmetric stretching vibration. The band at 1,630 cm⁻¹ was C—O or C—C stretching vibration, while the band at 1,373 cm⁻¹ was C—H stretching vibration and band 1,096 cm⁻¹ was —OH characteristic absorption peaks [14,15]. These results indicated that the CA had multiple oxygencontaining functional groups. Furthermore, XPS was also verified the existence of large number of oxygen-containing functional groups on the surface of CA, such as —OH, —COOH. There were

three fitted peak in C 1s spectrum (Fig. S2d online) positioned at 284.2, 286.5 and 288.0 eV, representing C—C, C—O and C=O respectively. Similarly, the O 1s had two peaks positioned at 531.8 and 533.0 eV, referring to C=O and C—O respectively (Fig. S2c online) [28]. From the above analysis, the negatively charged oxygen-containing functional groups (—OH, —COOH) would catch the metal ions under the electrostatic force when the metal ions diffused into CA during the flowing of solution, so that the CoNiAl-LDH can in situ formed on the surface of CA.

To explore the application of CoNiAl-LDH@CA in supercapacitor, cyclic voltammograms and galvanostatic charging-discharging in the potential range of 0.15–0.55 V in 2 mol/L KOH aqueous solution with a three-electrode system was conducted. Fig. 4a shows the CV measurement results at different scanning rates varying from 5 to 100 mV/s. The area of the curve was increased gradually from 5 mV/s to 100 mV. The asymmetric of CV curves suggested that the observed capacity mainly results from the pseudocapacitance, from 1 to 10 A/g, the discharge time decreased gradually, which is based on the reversible redox mechanism of CoNiAl-LDH. The charge-discharge reactions of the CoNiAl-LDH are as followings [33]:

$$Co(OH)_2 + OH^- \leftrightarrow CoOOH + H_2O + e^-$$

$$Ni(OH)_2 + OH^- \leftrightarrow NiOOH + H_2O + e^-$$

The charging-discharge behavior was further tested at the current densities from 1 to 10 A/g (Fig. 4b). The shape of the curves showed a high degree of symmetry in charge and discharge, indicating that the columbic efficiency of CoNiAl-LDH@CA at various current densities was nearly 100%. The calculated specific capacitances were 1,134 F/g at 1 A/g and 902 F/g at 10 A/g, respectively, which were much higher than those of carbonaceous aerogel (176 F/g) or CoNiAl-LDH (836 F/g) alone at 1 A/g (Fig. S3 online). The specific capacitance of CoNiAl-LDH@CA was also comparable with those materials in the literatures (Table S1 online).

Electrochemical impedance spectroscopy (EIS) was carried out to study the enhanced electrical conductivity of CoNiAl-LDH@CA based electrode. The Nyquist plot was obtained ranging from 0.01 Hz to 0.1 MHz in 2 mol/L KOH solution. As shown in Fig. 4d, the inset image was the equivalent circuit model through EIS data fitting. R_s was relate to the resistance of the material and calculated to be only 4.4 Ω through the equivalent circuit model [14,34–36], suggesting that the CoNiAl-LDH@CA electrode had a high electronic conductivity. The durability of electron was also tested by charge-discharge at 10 A/g. As shown in Fig. 4e, the capacitance maintained about 96% (863 F/g) after 4,000 cycles. As shown in the Fig. S4 (online), the structure of CoNiAl-LDH@CA has no obviously change after the cycles. Moreover, the columbic efficiency was nearly 100% during the charge-discharge processes. The high stability of electrode was due to the robust structure of CA that supported the transport of electron between electrolyte and active material.

These results demonstrate high specific capacitance and excellent cycling property of CoNiAl-LDH@CA as electrode material for high-performance electrochemical pseudo capacitor. The excellent performance of CoNiAl-LDH@CA can be attributed to the following reasons: CoNiAl-LDH nanoplates perpendicularly grown on CA facilitates the electrolyte accessible to the electro active sites on the composite (Fig. S4 online), which will shorten the ion transport distance and enhance the rate of redox reaction. Moreover, CA has good electronic conductivity and serves as a conductive matrix to provide conductive networks for electron transport during the electrode reaction processes.

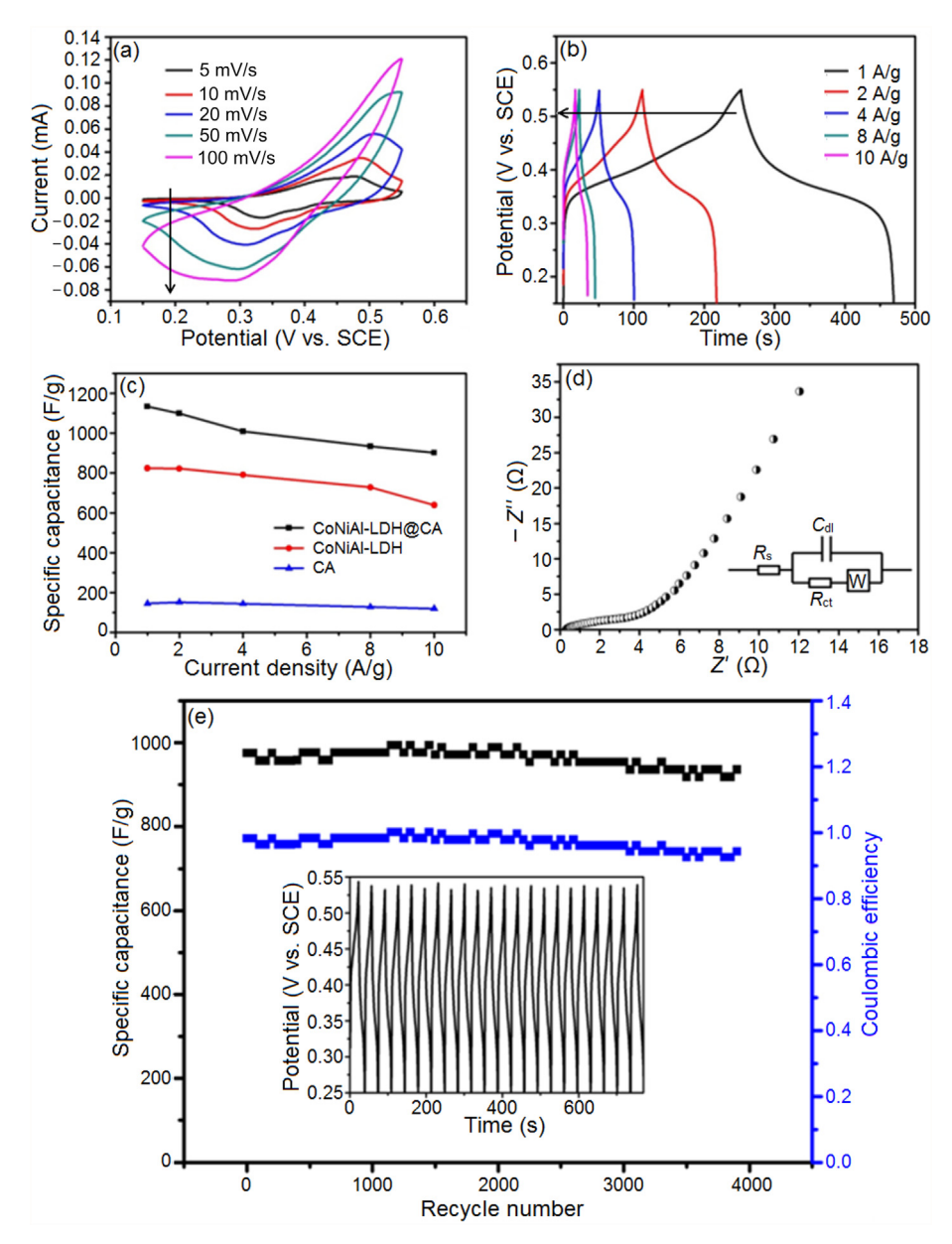


Fig. 4. (Color online) Electrochemical measurement of CoNiAl-LDH@CA in 2 mol/L KOH solution. (a) CV curves, (b) galvanostatic charging-discharge curves, (c) specific capacitances, (d) Nyquist curve, and (e) cycle properties at 10 A/g (the inset is the charge/discharge curves of the CoNiAl-LDH@CA electrode).

4. Conclusions

We have developed a two-step hydrothermal route to prepare CoNiAl-LDH@CA composites from waste biomass. When used as an electrode material for supercapacitor, CoNiAl-LDH@CA exhibited high specific capacitances of 1,134 F/g at 1 A/g and 902 F/g at 10 A/g, respectively. Furthermore, they displayed an excellent cycling stability without an obvious capacitance decrease after 4,000 cycles. The excellent electrochemical properties can be ascribed to the special structure CoNiAl-LDH nanoplates perpendicularly grown on CA, as well as the good electrical conductivity of CA, making it a highly promising electrodes in pseudocapacitor.

Conflict of interest

The authors declare that they have no conflict of interest.

Acknowledgments

This work was supported by the National Natural Science Foundation of China (21333009, 21273244, 21573245) and the Youth Innovation Promotion Association of Chinese Academy of Sciences (2017049).

Appendix A. Supplementary data

Supplementary data associated with this article can be found, in the online version, at http://dx.doi.org/10.1016/j.scib.2017.05.019.

References

[1] Wei TY, Chen CH, Chien HC, et al. A cost-effective supercapacitor material of ultrahigh specific capacitances: spinel nickel cobaltite aerogels from an epoxide-driven sol-gel process. Adv Mater 2010;22:347–51.

- [2] Zhang J, Yao Y, Liu J. Autonomous convergence and divergence of the self-powered soft liquid metal vehicles. Sci Bull 2015;60:943–51.
- [3] Zhai Y, Dou Y, Zhao D, et al. Carbon materials for chemical capacitive energy storage. Adv Mater 2011;23:4828–50.
- [4] Zhao L, Fan LZ, Zhou MQ, et al. Nitrogen-containing hydrothermal carbons with superior performance in supercapacitors. Adv Mater 2010;22:5202–6.
- [5] Wu XL, Xu AW. Carbonaceous hydrogels and aerogels for supercapacitors. J Mater Chem A 2014;2:4852–64.
- [6] Liu WJ, Tian K, He YR, et al. High-yield harvest of nanofibers/mesoporous carbon composite by pyrolysis of waste biomass and its application for high durability electrochemical energy storage. Environ Sci Technol 2014:48:13951-9.
- [7] Jin Z, Yan X, Yu Y, et al. Sustainable activated carbon fibers from liquefied wood with controllable porosity for high-performance supercapacitors. J Mater Chem A 2014;2:11706.
- [8] Salinas-Torres D, Lozano-Castelló D, Titirici MM, et al. Electrochemical behaviour of activated carbons obtained via hydrothermal carbonization. J Mater Chem A 2015;3:15558–67.
- [9] Liu J, Deng Y, Li X, et al. Promising nitrogen-rich porous carbons derived from one-step calcium chloride activation of biomass-based waste for high performance supercapacitors. ACS Sust Chem Eng 2016;4:177–87.
- [10] Bazaka K, Jacob MV, Ostrikov KK. Sustainable life cycles of natural-precursorderived nanocarbons. Chem Rev 2016;116:163–214.
- [11] Zhao SL, Li YC, Yin HJ, et al. Three-dimensional graphene/Pt nanoparticle composites as freestanding anode for enhancing performance of microbial fuel cells. Sci Adv 2015;1:e1500372.
- [12] Li XQ, Chang L, Zhao SL, et al. Research on carbon-based electrode materials for supercapacitors. Acta Phys Chim Sin 2017;33:130–48.
- [13] Candelaria SL, Cao G. Increased working voltage of hexamine-coated porous carbon for supercapacitors. Sci Bull 2015;60:1587–97.
- [14] Wu XL, Wen T, Guo HL, et al. Biomass-derived sponge-like carbonaceous hydrogels and aerogels for supercapacitors. ACS Nano 2013;7:3589–97.
- [15] Liang Q, Ye L, Huang ZH, et al. A honeycomb-like porous carbon derived from pomelo peel for use in high-performance supercapacitors. Nanoscale 2014;6:13831-7.
- [16] Li J, Liu K, Gao X, et al. Oxygen- and nitrogen-enriched 3D porous carbon for supercapacitors of high volumetric capacity. ACS Appl Mater Interfaces 2015;7:24622-8.
- [17] Song S, Ma F, Wu G, et al. Facile self-templating large scale preparation of biomass-derived 3D hierarchical porous carbon for advanced supercapacitors. J Mater Chem A 2015;3:18154–62.
- [18] Madhu R, Veeramani V, Chen SM, et al. Honeycomb-like porous carbon-cobalt oxide nanocomposite for high-performance enzymeless glucose sensor and supercapacitor applications. ACS Appl Mater Interfaces 2015;7:15812–20.
- [19] Yu C, Yang J, Zhao C, et al. Nanohybrids from NiCoAl-LDH coupled with carbon for pseudocapacitors: understanding the role of nano-structured carbon. Nanoscale 2014;6:3097–104.
- [20] Hatui G, Nayak GC, Udayabhanu G. One pot solvothermal synthesis of sandwich-like Mg Al layered double hydroxide anchored reduced graphene

- oxide: an excellent electrode material for supercapacitor. Electrochim Acta 2016:219:214-26.
- [21] Peng W, Li H, Song S. Synthesis of fluorinated graphene/CoAl-layered double hydroxide composites as electrode materials for supercapacitors. ACS Appl Mater Interfaces 2017;9:5204–12.
- [22] Huang P, Cao C, Sun Y, et al. One-pot synthesis of sandwich-like reduced graphene oxide@CoNiAl layered double hydroxide with excellent pseudocapacitive properties. | Mater Chem A 2015;3:10858–63.
- [23] Diao ZP, Zhang YX, Hao XD, et al. Facile synthesis of CoAl-LDH/MnO₂ hierarchical nanocomposites for high-performance supercapacitors. Ceramics Int 2014;40:2115–20.
- [24] Hao X, Zhang Y, Diao Z, et al. Engineering one-dimensional and two-dimensional birnessite manganese dioxides on nickel foam-supported cobalt-aluminum layered double hydroxides for advanced binder-free supercapacitors. RSC Adv 2014;4:63901–8.
- [25] Deng J, Xiong T, Xu F, et al. Inspired by bread leavening: one-pot synthesis of hierarchically porous carbon for supercapacitors. Green Chem 2015;17:4053-60.
- [26] Genovese M, Jiang J, Lian K, et al. High capacitive performance of exfoliated biochar nanosheets from biomass waste corn cob. J Mater Chem A 2015;3:2903–13.
- [27] Ma F, Wan J, Wu G, et al. Highly porous carbon microflakes derived from catkins for high-performance supercapacitors. RSC Adv 2015;5:44416–22.
- [28] Qie L, Chen W, Xu H, et al. Synthesis of functionalized 3D hierarchical porous carbon for high-performance supercapacitors. Energy Environ Sci 2013;6:2497.
- [29] Shen Y. Carbothermal synthesis of metal-functionalized nanostructures for energy and environmental applications. J Mater Chem A 2015;3:13114–88.
- [30] Liang HW, Guan QF, Chen LF, et al. Macroscopic-scale template synthesis of robust carbonaceous nanofiber hydrogels and aerogels and their applications. Angew Chem Int Ed 2012;51:5101–5.
- [31] Ren Y, Xu Q, Zhang J, et al. Functionalization of biomass carbonaceous aerogels: selective preparation of MnO₂@CA composites for supercapacitors. ACS Appl Mater Interfaces 2014;6:9689–97.
- [32] He L, Liu Y, Liu J, et al. Core-shell noble-metal@metal-organic-framework nanoparticles with highly selective sensing property. Angew Chem 2013;52:3741–5.
- [33] Zhao SL, Yin HJ, Du L, et al. Carbonized nanoscale metal-organic frameworks as high performance electrocatalyst for oxygen reduction reaction. ACS Nano 2014;8:12660–8.
- [34] Zhao SL, Wang Y, Dong JC, et al. Ultrathin metal-organic framework nanosheets for electrocatalytic oxygen evolution. Nat Energy 2016;1:1–10.
- [35] Yin HJ, Tang ZY. Ultrathin two-dimensional layered metal hydroxides: an emerging platform for advanced catalysis, energy conversion and storage. Chem Soc Rev 2016;45:4873–91.
- [36] Tang H, Wang J, Yin H, et al. Growth of polypyrrole ultrathin films on MoS₂ monolayers as high-performance supercapacitor electrodes. Adv Mater 2015;27:1117–23.